Defence Research and Development Canada
Recherche et développement pour la défense Canada

DEFENCE R&D DÉFENSE

A New Approach in Time-Frequency Analysis with Applications to Experimental High Range Resolution Radar Data

T. Thayaparan and G. Lampropoulos

Defence R&D Canada – Ottawa
TECHNICAL REPORT
DRDC Ottawa TR 2003-187
November 2003

Canada

A New Approach in Time-Frequency Analysis with Applications to Experimental High Range Resolution Radar Data

T. Thayaparan
Defence R&D Canada - Ottawa

G. Lampropoulos
A.U.G. Signals Ltd.

Defence R&D Canada - Ottawa

Technical Report

DRDC Ottawa TR 2003-187

November 2003

Abstract

This report presents trade-off studies on Time-Frequency Distribution (TFD) algorithms and a methodology for fusing them to achieve better target characterization. It is shown that TFD algorithmic fusion considerably increases the detectability of signals while suppressing artifacts and noise. The report reviews a sample of representative TFD algorithms. Their performance is studied from a qualitative and quantitative point of view. For simplicity, we considered the mean-squared error as a measure of performance in the quantitative trade-off studies. The TFD algorithmic fusion is performed using a self-adaptive signal. It may be adjusted to work for a wide range of signal-to-noise ratios. The algorithm uses the first two terms of the Volterra series expansion and we treat the outputs of the time-frequency algorithms as the variables of a Volterra series and the coefficients of the series are estimated through training sets with a least-squares algorithm. Simplistic TFD algorithmic fusion methods (e.g., weighted averaging or weighted multiplication) are special cases of the proposed fusion technique. We demonstrate the effectiveness of TFD algorithmic fusion method using experimental High Range Resolution (HRR) radar data and simulated data.

Résumé

Le présent rapport décrit des études de compromis portant sur les algorithmes de distribution temps-fréquence (DTF) et une méthode permettant de les fusionner en vue d'accroître la performance. On montre que la fusion d'algorithmes de DTF accroît considérablement la détectabilité des signaux tout en supprimant les artefacts et le bruit. Le rapport examine un échantillon d'algorithmes de DTF représentatifs. Leur performance est étudiée des points de vue qualitatif et quantitatif. Par souci de simplicité, nous avons utilisé l'erreur quadratique moyenne comme mesure de la performance dans les études de compromis quantitatives. On effectue la fusion des algorithmes de DTF en utilisant un signal auto-adaptatif. Un ajustement peut être effectué pour l'utilisation avec une vaste gamme rapports signal/bruit. En utilisant les deux premiers termes du développement en série de Volterra, nous traitons les résultats des algorithmes temps-fréquence comme les variables d'une série de Volterra, et les coefficients de la série sont évalués au moyen d'ensembles d'entraînement par un algorithme des moindres carrés. Les méthodes simples de fusion des algorithmes de DTF (p. ex. moyennage pondéré ou multiplication pondérée) sont des cas particuliers de la technique de fusion proposée. Nous démontrons l'efficacité de la méthode de fusion des algorithmes de DTF en nous servant de données expérimentales du radar à haute résolution en distance (HRR).

Executive summary

One of the most serious deficiencies in NATO's air defence capability and the one that affects almost every aspect of air command and control, and weapon systems are the lack of a rapid and reliable means of identifying air targets. Radar offers a capability to identify targets over long distances, under all weather conditions, during day or night, without the need for the target's cooperation. This mode of identification is known as Non-Cooperative Target Recognition (NCTR). The problem of NCTR has always been a topic of interest in military operations, that is, to improve situational awareness.

The radar echo provides a target profile that serves as a 'signature' for identification purposes. There are a number of radar techniques that can be applied to NCTR. Among some of the more promising methods are High Range Resolution (HRR), Jet Engine Modulation (JEM) and Inverse Synthetic Aperture Radar (ISAR). An operational NCTR system must satisfy two requirements: accurate identification and real time operation. It has been identified that HRR would be a promising candidate for an operational NCTR system. HRR has a relatively simple structure (e.g., 1-dimensional imagery) and has an all aspect capability. It requires a modest signal-to-noise ratio, and is applicable to a large class of radar systems.

Our previous experimental studies show that HRR radar image profiles can be severely distorted when a target possesses very small-perturbed random motions. Therefore the ability to generate focussed images from HRR is of paramount importance to military and intelligence operations. One of the central problems in HRR radar data is the analysis of a time series. Traditionally, HRR radar signals have been analysed in either the time or the frequency domain. The Fourier transform is at the heart of a wide range of techniques that are used in HRR radar data analysis and processing. The Fourier transform-based techniques are effective as long as the frequency contents of the signal do not change with time. However, the change of frequency content with time is one of the main features we observe in HRR radar data. Because of this change of frequency content with time, HRR radar signals belong to the class of non-stationary signals. Consequently, for the interpretation of radar data in terms of a changing frequency content, we need a representation of our data as a function of both time and frequency. Time-Frequency Distributions (TFDs) describe signals in term of their joint time-frequency content. These distributions are useful for analyzing signals with both time and frequency variations. Therefore, for signals with time-varying frequency contents, TFDs offer a powerful analysis tool. Analysis of the time-varying Doppler signature in the joint time-frequency domain can provide useful information for target detection, classification and recognition.

In this report, a new TFD algorithmic fusion method has been presented and evaluated on experimental HRR radar data and simulated data. It is shown that our TFD algorithmic fusion method provides an effective method of achieving improved resolution, highly concentrated and readable representation without the auto-term distortion and cross-term artifacts. This method is suitable for HRR and ISAR data

where multiple scatterers are present, and that noise and artifact reduction are essential for target identification applications. Analysis of the time-varying Doppler signature in the joint time-frequency domain can provide useful information for target detection, classification and recognition. We anticipate that this new approach will find a wide range of uses and will emerge as a powerful tool for time-varying spectral analysis.

This study is a part of the work sponsored by the US Office of Naval Research to investigate the distortion of HRR and ISAR images under the US Navy's International Collaborative Opportunity Program (NICOP). Canada is a participant in this project on "Time-frequency processing for ISAR imaging and Non-Cooperative Target Identification". The work performed in this report is relevant to the ISAR imaging capability of the surveillance radar systems on-board of the CF C-140 Aurora patrol aircraft. It should also be noted that target recognition based on radar imagery will play an important role in future CF initiatives on ISR (Intelligence, Surveillance and Reconnaissance) for land, air and maritime applications.

T. Thayaparan , G. Lampropoulos. 2003. A New Approach in Time-Frequency Analysis with Applications to Experimental High Range Resolution Radar Data. DRDC Ottawa TR 2003-187. Defence R&D Canada - Ottawa.

Sommaire

Une des plus graves lacunes de la capacité de défense aérienne de l'OTAN, qui a une incidence sur presque tous les aspects du commandement et du contrôle aériens ainsi que des systèmes d'armes, est l'absence d'un moyen rapide et fiable d'identification des objectifs aériens. Le radar permet d'identifier les objectifs sur de grandes distances, dans toutes les conditions météorologiques, le jour ou la nuit, sans nécessiter la coopération de l'objectif. Ce mode d'identification est appelé la reconnaissance de cible non coopérative (NCTR). Le problème de la NCTR a toujours présenté un intérêt dans les opérations militaires, par exemple du point de vue de l'amélioration de la connaissance de la situation.

L'écho radar fournit un profil d'objectif qui sert de « signature » aux fins de l'identification. Il existe un certain nombre de techniques radar qui peuvent être appliquées à la NCTR. La technique à haute résolution en distance (HRR), la modulation des moteurs à réaction (JEM) et la technique du radar à synthèse d'ouverture inverse (ISAR) comptent parmi les méthodes les plus prometteuses. Un système de NCTR opérationnel doit satisfaire à deux exigences : identification précise et fonctionnement en temps réel. On a déterminé que la technique HRR serait une candidate prometteuse comme système de NCTR opérationnel. Elle comporte une structure relativement simple (p. ex. imagerie unidimensionnelle) et elle possède une capacité tous secteurs. Il lui suffit d'un faible rapport signal/bruit et elle est applicable à une large classe de systèmes radar.

Nos études expérimentales antérieures montrent que les profils d'images obtenus avec le radar HRR peuvent être fortement déformés lorsqu'un objectif effectue des mouvements aléatoires très faiblement perturbés. Par conséquent, la capacité de générer des images mises au point à partir du radar HRR est d'une importance primordiale pour les opérations militaires et les opérations de renseignement. L'analyse d'une série chronologique constitue l'un des principaux problèmes éprouvés avec les données du radar HRR. Par le passé, les signaux radar ont été analysés soit dans le domaine temporel, soit dans le domaine fréquentiel. La transformation de Fourier est au cœur d'une vaste gamme de techniques qui sont utilisées pour l'analyse et le traitement des données du radar HRR. Les techniques à transformation de Fourier sont efficaces dans la mesure où le contenu fréquentiel du signal ne varie pas avec le temps. Cependant, la variation du contenu fréquentiel avec le temps est une des principales caractéristiques que nous observons dans les données du radar HRR. En raison de cette variation du contenu fréquentiel avec le temps, les signaux du radar HRR appartiennent à la catégorie des signaux non stationnaires. Par conséquent, pour l'interprétation des données radar du point de vue d'un contenu fréquentiel changeant, nous avons besoin d'une représentation de nos données en fonction du temps et de la fréquence. Les distributions temps-fréquence(DTF) décrivent les signaux du point de vue de leur contenu temporel-fréquentiel. Elles sont utiles pour l'analyse des signaux qui présentent des variations temporelles et fréquentielles. Par conséquent, les DTF constituent un outil d'analyse puissant des signaux dont le contenu fréquentiel varie

dans le temps.

Dans ce rapport, nous avons présenté une nouvelle méthode de fusion des algorithmes de DTF et nous l'avons évaluée en l'appliquant aux données expérimentales du radar HRR. On montre que la méthode de fusion des algorithmes de DTF constitue un moyen efficace pour obtenir une représentation à résolution accrue, hautement concentrée et lisible sans la distorsion des auto-termes ni les artefacts de termes croisés. Cette méthode est applicable aux données du radar HRR et du radar ISAR lorsque des diffuseurs multiples sont présents, et que la réduction du bruit et des artefacts est essentielle pour les applications d'identification d'objectif. Nous espérons que cette nouvelle approche aura aussi des applications dans une vaste gamme de situations et qu'elle se révélera un outil puissant pour l'analyse des spectres variant dans le temps.

T. Thayaparan , G. Lampropoulos. 2003. A New Approach in Time-Frequency Analysis with Applications to Experimental High Range Resolution Radar Data. DRDC Ottawa TR 2003-187. R & D pour la défense Canada - Ottawa.

Table of contents

List of figures

1. Introduction

Our previous experimental studies show that High Range Resolution (HRR) radar image profiles can be severely distorted when a target possesses very small-perturbed random motions [1]. The ability to generate focussed images from HRR is of paramount importance to military and intelligence operations. One of the central problems in HRR radar data is the analysis of a time series. Traditionally, HRR radar signals have been analysed in either the time or the frequency domain. The Fourier transform is at the heart of a wide range of techniques that are used in HRR radar data analysis and processing. The Fourier transform-based techniques are effective as long as the frequency contents of the signal do not change with time [2-3]. However, the change of frequency content with time is one of the main features we observe in HRR radar data when stepped frequency wave form HRR processing is used. Because of this change of frequency content with time, HRR radar signals belong to the class of non-stationary signals. Consequently, for the interpretation of radar data in terms of a changing frequency content, we need a representation of our data as a function of both time and frequency. Time-Frequency Distributions (TFDs) describe signals in term of their joint time-frequency content. These distributions are useful for analyzing signals with both time and frequency variations. Therefore, for signals with time-varying frequency contents, TFDs offer a powerful analysis tool.

Over the past ten years, radar researchers have also investigated TFDs as a unique tool for radar-specific signal analysis and image processing applications [4-10]. It was found that TFDs provide additional insight into the analysis, interpretation, and processing of radar signals that are sometimes superior to what is achievable in the traditional time or frequency domain alone. The specific applications where TFDs have been used include signal analysis and feature extraction, motion compensation and image formation, signal SNR (signal-to-noise ratio) improvement, imaging of moving targets, and detection of moving targets [4-10].

The most widely known time-frequency analysis techniques belong to the Cohen class with the leading transform being the Wigner-Ville distribution, which is based on a bilinear model [5-7,11-12]. This model is able to analyze time-varying signals with relatively high resolution. However, being a bilinear model it introduces cross-term artifacts[5-7,11-12]. Hence, filtering techniques have been proposed to reduce the cross-term artifacts. Among them, the most well known filtering method uses the Choi-Williams filter [13]. Higher than bilinear order models have also been proposed for time-frequency analysis, e.g., Wigner bispectrum and trispectrum. Choi-Williams filters have also been incorporated into these models. These higher-order models work well with isolated signals (time-varying or stationary). However, it will be shown in this report that it is very difficult to reduce the cross-term artifacts in the case of multiple signals (i.e., multiple point scatterers from a target).

Wavelet-based transforms have been also proposed for time-frequency analysis. Wavelet transforms break the signal into a set of bases with a shape that is based on

affine transformations (i.e., translations and dilations) of a basic wavelet called the mother wavelet. Here the aspect ratios in the time-frequency plane are proportional to the distance from the zero frequency and the ratio of the bandwidth to the center frequency remains constant [4]. Among the most simple but also effective time-frequency wavelets is the Gabor based time-frequency expansion, where the mother wavelet is a Gaussian function. The Gabor transform originally used rectangles to designate each of the time-frequency elementary signals. Wavelet-based time-frequency analysis belongs to the Weyl-Hiesenberg generalized class. The introduction of chirplets for time-frequency analysis also belongs to the same class and has been used to better describe the second- (i.e. Doppler acceleration) and higher-order signal nonlinearity [5,14-15]. Another transform that is also considered as a generalization of the Gabor transform is the s-transform [16-17]. All these transforms do not introduce cross-term artifacts as those of the Cohen class time-frequency analysis methods. However, they often result in inferior resolution when compared to the Cohen class transforms.

Other techniques in time-frequency analysis include the Adaptive Joint Time-Frequency (AJTF) transform [8-9,18-19]. It is based on the series analysis of a time-varying signal into a high-order polynomial of time (i.e., Doppler, Doppler acceleration, etc.). The estimation of parameters assumes the presence of very strong (i.e., high signal-to-noise ratio) point scatterers. For example, for a second-order polynomial, at least two very strong scatterers are required from the same moving target. These polynomial parameters may be used for motion compensation as well as for target recognition.

In recent years the Fractional Fourier Transform (FRFT) has been introduced. The FRFT is able to find linear changes in the frequency over time [8]. However, for higher-order nonlinearity, extensions of this transform to time-frequency domain must be incorporated [14].

Enhancements and filtering techniques on the results of the above mentioned transforms have been proposed by many researchers. The most promising methods are the Choi-Williams filters which are applied in the Wigner-Ville class of time-frequency transforms and the reassignment methods, which are applied to any time-frequency distribution [20-21].

In this report we present a new method for increasing the detectability of time-varying signals, for high resolution improvements on the results and for reduction of the noise and cross-term artifacts. This new concept of time-frequency analysis is based on TFD algorithmic fusion. TFD algorithmic fusion is required to mathematically analyze the TFD algorithms. This analysis may be performed a priori, or, by using self-adaptive data analysis techniques on the results (e.g., by applying weighting techniques, where the weights are found optimally from training data sets using least-squares techniques or neural networks).

2. Time-Frequency Analysis Algorithms

In this section we present a sample of algorithms used in our performance evaluation and the development of an algorithmic fusion method to enhance the results. Detailed description, properties and derivation of each transform can be found from the references, particularly from [4-13].

2.1 Adaptive Energy Distribution (AED)

Adaptive Energy Distribution (AED) is a window-matched spectrogram, where the window matching is performed with the use of generalized instantaneous parameters (GIP's). The GIP's that are used for Gaussian window matching are the instantaneous time variance (ITV), the instantaneous frequency variance (IFV), and the instantaneous time-frequency (ITF) covariance [22]. These variance measures are calculated from instantaneous moments and expressed in the following succinct forms, i.e.,

$$ITV_{zh}(t,f) = -\frac{1}{8\pi^2}\,\Re\left[\frac{\partial^2 S_x(t,f)}{\partial f^2}\,\frac{1}{S_x(t,f)} - \left(\frac{\partial S_x(t,f)}{\partial f}\,\frac{1}{S_x(t,f)}\right)^2\right] \tag{1}$$

$$IFV_{zh}(t,f) = -\frac{1}{8\pi^2}\,\Re\left[\frac{\partial^2 S_x(t,f)}{\partial t^2}\,\frac{1}{S_x(t,f)} - \left(\frac{\partial S_x(t,f)}{\partial t}\,\frac{1}{S_x(t,f)}\right)^2\right] \tag{2}$$

$$ITF_{zh}(t,f) = -\frac{1}{8\pi^2}\Re\left[\frac{\partial^2 S_x(t,f)}{\partial f \partial t}\frac{1}{S_x(t,f)} - \frac{\partial S_x(t,f)}{\partial f}\frac{\partial S_x(t,f)}{\partial t}\left(\frac{1}{S_x(t,f)}\right)^2\right] \tag{3}$$

where $S_x(t,f)$ specifies the spectrogram of the signal $x(t)$ formed using the window $h(t)$. $\Re$ indicates the real part of the expression and $f = \omega/(2\pi)$, where f is the frequency and ω is the angular frequency. The subscript zh in equations (1)-(3) denotes that the signal $x(t)$ has been multiplied by the window $h(t)$. The parameters for an optimal window are found by matching the GIP's of the signal-window spectrogram to those of the window-window spectrogram. The optimal window parameters are updated iteratively until the desired level of matching is achieved. At the n^{th} iteration they are calculated with

$$\alpha_{n+1}(t,f) = \frac{(8\pi)^3\,(ITF_{zh_n}(t,f))^2\,IFV_{zh_n}(t,f)}{(8\pi)^2\,(ITF_{zh_n}(t,f))^2 + 1} \tag{4}$$

and

$$\beta_{n+1}(t,f) = \frac{(8\pi)^2\, ITF_{zh_n}(t,f)\, IFV_{zh_n}(t,f)}{(8\pi)^2\, (ITF_{zh_n}(t,f))^2 + 1} \tag{5}$$

or if $ITV_{zh_n}(t,f) > IFV_{zh_n}(t,f)$ then

$$\alpha_{n+1}(t,f) = \frac{1}{8\pi \cdot ITV_{zh_n}(t,f)} \tag{6}$$

and

$$\beta_{n+1}(t,f) = \frac{1}{(8\pi)^2\, ITV_{zh_n}(t,f)\, ITF_{zh_n}(t,f)} \tag{7}$$

where α and β are the parameters of the Gaussian window $h(t) = \exp^{-\pi(\alpha - j\beta)t^2}$.

2.2 Adaptive Gaussian Chirplet Decomposition (AGCD)

Adaptive joint time-frequency analysis is a good tool to analyze the time-varying Doppler features of a target. The chirp function is one of the most fundamental functions in nature. Many natural events, for example, signals in seismology and radar systems, can be modelled as a superposition of short-lived chirp functions. Hence, the chirp-based signal representation, such as the Gaussian chirplet decomposition, has been an active research area in the field of signal processing [4,15]. The Gaussian chirplet is defined as

$$h_k(t) = \sqrt[4]{\frac{\alpha_k}{\pi}}\, \exp\left\{-\frac{\alpha_k}{2}\,(t-t_k)^2 + j\,\left(\omega_k + \frac{\beta_k}{2}\,(t-t_k)\right)\,(t-t_k)\right\} \tag{8}$$

where $\alpha_k > 0$ and $t_k, \omega_k, \beta_k \varepsilon R$. $h_k(t)$ has a very short and smooth envelope, i.e., a Gaussian envelope. (t_k, ω_k) indicates the time and frequency center of the linear chirp function. The variance α_k controls the width of the chirp function. The parameter β_k determines the rate of change of frequency. It shows that not only can we adjust the variance and time-frequency center, but also we can regulate the orientation of $h_k(t)$ in the time-frequency domain by varying parameter β_k. For the Gaussian chirplet decomposition, the corresponding adaptive spectrogram is

$$AS(t,\omega) = 2\sum_k\, |B_k|^2\, \exp\left[-\alpha_k\,(t-t_k)^2 - \frac{1}{\alpha_k}\,(\omega - \omega_k - \beta_k t)^2\right] \tag{9}$$

which is non-negative. AGCD has an excellent resolution and has no cross-term artifacts.

2.3 Adaptive Gabor Expansion (AGE)

Adaptive Gabor Expansion (AGE) is similar to the adaptive Gaussian chirplet decomposition [4,15]. The only difference is AGE uses a Gaussian function instead of a Gaussian chirplet function, i.e.,

$$(10)\quad h_k(t) = \sqrt[4]{\frac{\alpha_k}{\pi}}\,\exp\left\{-\frac{\alpha_k}{2}\,(t-t_k)^2 + j\,\omega_k\,(t-t_k)\right\} \qquad t_k, \omega_k \varepsilon R, \alpha_k \varepsilon R^+$$

2.4 Linear Time-Frequency Transforms

All linear time-frequency transforms satisfy the superposition or linearity principle which states that if $x(t)$ is a linear combination of some signal components, then the time-frequency transforms of $x(t)$ have the same linear combination of the time-frequency transforms of each of the signal components, i.e.,

$$(11)\qquad x(t) = c_1\,x_1(t) + c_2\,x_2(t) \rightarrow T_x(t,f) = c_1\,T_{x_1}(t,f) + c_2\,T_{x_2}(t,f)$$

Linearity is a desirable property in any application involving multi component signals. One of the basic linear time-frequency transforms is the short-time Fourier transform (STFT) [5-7,10]. The STFT is given as

$$(12)\qquad STFT_x(t,\omega) = \int x(\tau)\,w(\tau - t)\,\exp(-j\omega\tau)\,d\tau$$

where $w(t)$ is a rectangular window function, t is time and τ is running time. When a Gaussian window is used, the result is the Gabor transform and is given as

$$(13)\qquad GTFT_x(t,\omega) = x(\tau)\,\frac{1}{\sqrt{\pi\sigma}}\,\exp\left\{-\frac{(\tau-t)^2}{2\sigma^2}\right\}\,\exp(-j\omega\tau)\,d\tau$$

where σ is the standard deviation. Other windowing functions that are used in this report are [5-7]:

$$(14)\qquad \text{Triangular window}: \quad w(t) = 1 - \frac{2|t|}{\tau} \quad \text{for} \quad |t| \le \frac{\tau}{2},$$

$$(15)\qquad \text{Hanning window}: \quad w(t) = \frac{1}{2}\left(1 + \cos\frac{2\pi t}{\tau}\right) \quad \text{for} \quad |t| \le \frac{\tau}{2},$$

$$\text{(16)} \qquad \text{Hamming window}: \quad w(t) = 0.54 + 0.46\,\cos\frac{2\pi t}{\tau} \quad \text{for} \quad |t| \le \frac{\tau}{2},$$

$$\text{(17)} \qquad \text{Blackman window}: \quad w(t) = 0.42 - 0.5\,\cos\frac{2\pi t}{\tau} + 0.08\,\cos\frac{2\pi t}{\tau} \quad \text{for} \quad |t| \le \frac{\tau}{2}.$$

$$\text{(18)} \qquad \text{Kaiser window}: \quad w(t) = \frac{I_0\left[\gamma\sqrt{1-(2t/\tau)^2}\right]}{I_0(\gamma)} \quad \text{for} \quad |t| \le \frac{\tau}{2},$$

where I_0 is the modified Bessel function of the first kind and of order zero, and γ is a parameter. We also introduce and test an inverse relation window function. Its amplitude response relatively has a narrow main-lobe and has almost no side-lobes. The inverse window function is given as

$$\text{(19)} \qquad \text{Inverse window function}: \quad w(t) = \left(\frac{1}{t+1}\right)^p \quad \text{for} \quad |t| \le \frac{\tau}{2}.$$

where the exponential p is a positive integer.

2.5 Bilinear Time-Frequency Distributions

In contrast to the linear time-frequency transforms such as the short-time Fourier transform, the Wigner-Ville distribution (WVD) is said to be bilinear. For a signal $s(t)$, its Wigner-Ville distribution is

$$\text{(20)} \qquad W_x(t,\omega) = \int x(t+\frac{\tau}{2})\,x^*(t-\frac{\tau}{2})\,\exp(-j\omega\tau)\,d\tau$$

The Wigner-Ville distribution not only possesses many useful properties, but also has better resolution than the STFT spectrogram. Although the Wigner-Ville distribution has existed for a long time, its applications are very limited. One main deficiency of the Wigner-Ville distribution is the so-called cross-term artifacts [5-7]. Suppose we express a signal as the sum of two signal components,

$$\text{(21)} \qquad x(t) = x_1(t) + x_2(t)$$

Substituting this into equation (20), we have

$$W_x(t,\omega) = W_{x_1x_1}(t,\omega) + W_{x_2x_2}(t,\omega) + W_{x_1x_2}(t,\omega) + W_{x_2x_1}(t,\omega) \tag{22}$$

where

$$W_{x_1x_2}(t,\omega) = \frac{1}{2\pi} \int x_1^\star(t - \frac{1}{2}\tau)\, x_2(t + \frac{1}{2}\tau)\, e^{-j\omega\tau}\, d\tau \tag{23}$$

This is called the cross Wigner-Ville distribution. In terms of the spectrum it is

$$W_{x_1x_2}(t,\omega) = \frac{1}{2\pi} \int x_1^\star(\omega + \frac{1}{2}\theta)\, x_2(\omega - \frac{1}{2}\theta)\, e^{-jt\theta}\, d\theta \tag{24}$$

The cross Wigner-Ville distribution is complex. However, $W_{x_1x_2} = W^\star_{x_2x_1}$, and therefore $W_{x_1x_2}(t,\omega) + W_{x_2x_1}(t,\omega)$ is real. Hence

$$W(t,\omega) = W_{x_1x_1}(t,\omega) + W_{x_2x_2}(t,\omega) + 2\,\Re\{W_{x_1x_2}(t,\omega)\} \tag{25}$$

We see that the Wigner-Ville distribution of the sum of the two signals is not the sum of the Wigner-Ville distribution of each signal but has the additional term $2\,\Re\{W_{x_1x_2}(t,\omega)\}$. The term is often called the interference term or the cross-term and it is often said to give rise to artifacts. Because the cross-term usually oscillates and its magnitude is twice as large as that of the auto-terms, it often obscures the useful time-dependent spectrum patterns.

The inverse Fourier transform of the Wigner-Ville distribution is called the ambiguity function (AF). The Fourier transform maps the Wigner-Ville distribution auto-terms to a region centered on the region of the AF plane, whereas it maps the oscillatory Wigner-Ville distribution cross-terms away from the origin [5-7,23-24].

The fact that the auto- and cross-terms are spatially separated in the AF domain means that if we apply a filter function to the AF, we can suppress some of the cross-terms. This filtering operation defines a new time-frequency distribution

$$\mathrm{TFD} = \mathrm{Fourier\ \ transform}\{\mathrm{AF} \cdot \mathrm{Kernel}\} \tag{26}$$

with properties different from the Wigner-Ville distribution. The filter function is called the ‘kernel’ of the TFD. Since there are many possible 2-dimensional kernel functions, there exist many different TFDs for the same signal. The class of all TFDs obtained in

this fashion is called Cohen's class. A more detailed description of the ambiguity function and Cohen's class are given [5-7,23-24].

Cohen's general class of bilinear TFDs is defined as

$$C(t,\omega) = \frac{1}{2\pi} \int \int \; AF(\theta,\tau)\, \Phi(\theta,\tau)\, \exp[j(\theta t - \omega\tau)]\, d\theta\, d\tau \tag{27}$$

where $\Phi(\theta,\tau)$ is a kernel function and $AF(\theta,\tau)$ is the ambiguity function of the signal defined by

$$AF(\theta,\tau) = \int \; x(t+\frac{\tau}{2})\, x^*(t-\frac{\tau}{2})\, \exp(-j\theta\tau)\, dt \tag{28}$$

where θ represents the frequency-offset and τ represents the time-offset. Cross-terms in the WVD can be effectively filtered in the ambiguity domain by designing kernels that filter the signal part of the ambiguity function. The kernel functions that are used in this report are [5-7]:

Born-Jordan:

$$\Phi(\theta,\tau) = 2\,\frac{\sin(\theta\tau/2)}{\theta\tau} \tag{29}$$

Choi-Williams:

$$\Phi(\theta,\tau) = \exp\left[-\frac{(\theta\tau)^2}{\sigma^2}\right] \tag{30}$$

Butterworth:

$$\Phi(\theta,\tau) = \left[1 + \left(\frac{\tau}{\tau_0}\right)^{2M} \left(\frac{\theta}{\theta_0}\right)^{2N}\right]^{-1} \tag{31}$$

Generalized exponential:

$$\Phi(\theta,\tau) = \exp\left[-\left(\frac{\tau}{\tau_0}\right)^{2M} \left(\frac{\theta}{\theta_0}\right)^{2N}\right]^{-1} \tag{32}$$

Cone-shaped,

(33) $$\Phi(\theta,\tau) = 2\,\exp(-\alpha\tau^2)\frac{\sin(\theta\tau/2)}{\theta}$$

Tilted Gaussian:

(34) $$\Phi(\theta,\tau) = \exp\left\{-\pi\left[\left(\frac{\tau}{\tau_0}\right)^2 + \left(\frac{\theta}{\theta_0}\right)^2 + 2r\left(\frac{\tau\theta}{\tau_0\theta_0}\right)\right]\right\}$$

Tilted Butterworth

(35) $$\Phi(\theta,\tau) = \left[1 + \left(\frac{\tau}{\tau_0}\right)^2 + \left(\frac{\theta}{\theta_0}\right)^2 + 2r\left(\frac{\tau\theta}{\tau_0\theta_0}\right)\right]^{-1}$$

where τ_0 and θ_0 are two scaling parameters and r is the rotation parameter. The kernel's contours are un-tilted when $r = 0$ and tilted ellipses when $r \neq 0$ in the AF plane. A tilted parallel strip is also possible by setting $r \pm 1$.

2.6 Adaptive Optimal-Kernel (AOK)

Since real signals have different shapes in the ambiguity domain, no single kernel can give adequate performance for a large class of signals. Hence, there has been increasing interest in signal-dependent or adaptive TFDs, in which the kernel function varies with the signal. Adaptation of the kernel over time is beneficial because it permits the kernel to match the local signal characteristics [25].

The signal-dependent TFR is based on kernels with Gaussian radial cross-sections

(36) $$\Phi(\theta,\tau) = \exp\left(-\frac{\theta^2+\tau^2}{2\sigma^2(\psi)}\right)$$

The function $\sigma(\psi)$ controls the spread of the Gaussian function at radial angle ψ. Clearly if σ is smooth, then Φ is smooth. The angle ψ is measured between the radial line through the point (θ,τ) and the θ-axis

(37) $$\psi = \arctan\frac{\tau}{\theta}$$

It is natural to express radially Gaussian kernels in polar coordinates; using $r = \sqrt{\theta^2+\tau^2}$ as the radius variable,

$$\Phi(r,\psi) = \exp\left(-\frac{r^2}{2\sigma^2(\psi)}\right). \tag{38}$$

A better TFD results when the kernel is well matched to the components of a given signal. The radially Gaussian kernel is adapted to a particular signal by solving the following optimization problem:

$$\max_{\Phi} \int_0^{2\pi} \int_0^{\infty} |AF(r,\psi)\,\Phi(r,\psi)|^2\, r\, dr\, d\psi \tag{39}$$

Subject to

$$\Phi(r,\psi) = \exp\left(-\frac{r^2}{2\sigma^2(\psi)}\right), \quad \int_0^{2\pi} \sigma^2(\psi)\, d(\psi) \leq \alpha, \quad \alpha \geq 0 \tag{40}$$

Here, $AF(r,\psi)$ is the AF of the signal in polar coordinates. The problem requires the area of the kernel to be constant with the projection of the kernel on the ambiguity function of the signal to be maximal. Since this optimization problem takes a long time to solve, a simplified adaptive kernel is implemented. The simplified adaptive kernel is just proportional to the sum of the ambiguity function in each radial direction, i.e.,

$$\sigma(\psi) = c \int_0^{\infty} |AF(r,\psi)|^2\, dr, \quad c \geq 0 \tag{41}$$

The parameter c is similar to α in equation (40) and determines the extent of the kernel in a radial direction. This way the kernel lets through most of the signal's auto-terms but not the cross-terms and calculates the optimization problem more quickly. An adaptive kernel, which is radially inverse, has been also proposed for the TFD, i.e.,

$$\Phi(r,\psi) = \left[1 + \left(\frac{r}{\sigma(\psi)}\right)^2\right]^{-1} \tag{42}$$

An adaptive kernel, which is radially constant, is also proposed for the TFD and is given as

$$\Phi(r,\psi) = \begin{cases} 1 & \text{if} \quad \exp\left(-\frac{r^2}{2\sigma^2(\psi)}\right) \geq k \\ 0 & \text{if} \quad \exp\left(-\frac{r^2}{2\sigma^2(\psi)}\right) < k \end{cases} \tag{43}$$

where k is a constant

3. Fusion of algorithms - A new approach

Fusion of TFD algorithms requires mathematical analysis of the performance of each algorithm under a wide range of single or multiple signals of interest at all signal-to-noise ratios and with noise models that are representative to the operating environment of applicability. The objective of fusing TFD algorithms is to develop a system that has better performance than any subset of algorithms or their combinations.

It is extremely difficult to develop a single TFD algorithm that produces satisfactory resolution and low noise levels with no cross-term artifacts for all signals and signal-to-noise ratios. However, different TFD may filter various components of signals with different degree of success, based on the quality and number of signals and their signal-to-noise ratios. With many TFD algorithms available a combination of them may result in both high resolution and low levels of noise and cross-term artifacts. TFD algorithmic fusion is designed to amplify results from algorithms that produce good TFDs and to suppress algorithms that do not work well for a particular environment.

Mathematical analysis of the TFD algorithms, for all kinds of environments, is not an easy task. In this section we present a methodology that weights the outputs of selected TFDs and their first-order multiplication (i.e. first- and second-order terms of a Volterra series expansion) to result in an enhanced TFD. The enhanced TFD produces high resolution, low cross-term artifacts and low noise. Herein, the presented fusion process produces a new TFD, which is a linear combination of the TFDs from available algorithms and their products.

The fusion process finds the coefficients ρ_l for each of the TFDs $A_l = \{a_{ij}\}_l$ of the available algorithms such that the linear combination is a close as possible to the ideal, noise free, TFD:

$$\rho_1 A_1 + \rho_2 A_2 + ... + \rho_n A_n = D \tag{44}$$

Equivalently equation (44) can be written as

$$\sum_{l=1...n} \rho_l (a_{ij})_l = d_{ij} \tag{45}$$

where $D = \{d_{ij}\}$ is the ideal distribution. In this description, n refers to the number of available time-frequency algorithms and their TFDs, and N is the length of a signal. To solve for $\underline{\rho}$ each A_l matrix is written as a column and the equation becomes

(46)
$$\begin{bmatrix} (a_{11})_1 & (a_{11})_2 & ... & (a_{11})_n \\ (a_{12})_1 & (a_{12})_2 & ... & (a_{12})_n \\ \vdots & \vdots & \ddots & \vdots \\ (a_{NN})_1 & (a_{NN})_2 & ... & (a_{NN})_n \end{bmatrix} \begin{bmatrix} \rho_1 \\ \rho_1 \\ \vdots \\ \rho_1 \end{bmatrix} = \begin{bmatrix} d_{11} \\ d_{12} \\ \vdots \\ d_{NN} \end{bmatrix}$$

which has the least-square solution

(47)
$$\underline{\rho} = [B^t B]^{-1} B^t \underline{c}$$

where B is the matrix that contains the TFDs of each algorithm as columns and $\underline{c}$ is the column vector that contains all the d_{ij}. Once all the coefficients ρ_l are known, a fused TFD F can be constructed according to

(48)
$$\rho_1 A_1 + \rho_2 A_2 + ... + \rho_n A_n = F$$

To include multiplications between the TFDs of different algorithms, equation (45) can be changed to

(49)
$$\sum_{l=1...n} \rho_l A_l + \sum_{i=1...n; j=i+1...n} \mu_{ij} A_i A_j = D$$

where $A_i A_j = \tilde{A}$ are element by element products between each pair of TFDs and μ_k are their coefficients in the fused TFD. With this modification, the matrix B will include the columns of A_l as well as $\tilde{A}_k$ and $\underline{\rho}$ will be a column vector with both ρ_l and μ_k in it. Solution of equation (47) will give the coefficients that are required to make the fused TFD. When multiplicative factors are included in the fusion process, the signal parts are amplified, and at the same time, blurring and artifacts are suppressed.

In order to make the fusion process to suppress noise (in addition to artifacts) in the TFDs of the given algorithms, the coefficients $\underline{\rho}$ have to include the noise information. When TFDs with different noise levels (SNR) are present, then a separate matrix B^{SNR_m} is formed for each SNR, i.e.,

(50)
$$B^{SNR_m} = \begin{bmatrix} (a_{11})_1^{SNR_m} & (a_{11})_2^{SNR_m} & .. & (a_{11})_n^{SNR_m} & (\tilde{a}_{11})_1^{SNR_m} & (\tilde{a}_{11})_2^{SNR_m} & .. & (\tilde{a}_{11})_{\frac{n^2-n}{2}}^{SNR_m} \\ (a_{12})_1^{SNR_m} & (a_{12})_2^{SNR_m} & .. & (a_{12})_n^{SNR_m} & (\tilde{a}_{12})_1^{SNR_m} & (\tilde{a}_{12})_2^{SNR_m} & .. & (\tilde{a}_{12})_{\frac{n^2-n}{2}}^{SNR_m} \\ \vdots & \vdots & \ddots & \vdots & \vdots & \vdots & \ddots & \vdots \\ (a_{NN})_1^{SNR_m} & (a_{NN})_2^{SNR_m} & .. & (a_{NN})_n^{SNR_m} & (\tilde{a}_{NN})_1^{SNR_m} & (\tilde{a}_{NN})_2^{SNR_m} & .. & (\tilde{a}_{NN})_{\frac{n^2-n}{2}}^{SNR_m} \end{bmatrix}$$

Then equation (46) becomes

$$\begin{bmatrix} B^{SNR_1} \\ B^{SNR_2} \\ \vdots \\ B^{SNR_M} \end{bmatrix} \underline{\rho} = \begin{bmatrix} \underline{c} \\ \underline{c} \\ \vdots \\ \underline{c} \end{bmatrix} \tag{51}$$

Solution of equation (51) can then be used to make a TFD in which noise and artifacts are suppressed. Equation (51) may be extended to include multiple signals and furthermore make the proposed approach applicable to a wider set of signals. It should be pointed out that equation (51) is used for the training process, where only the vector $\boldsymbol{\rho}$ is unknown. The left part of the equation (51) is used for the fusion process, when the signal is unknown.

Although the fusion process requires an ideal TFD in order to find the coefficients of each available distribution, it is required only once. After the coefficients are estimated, they are used to construct fused TFDs of signals from the same source, but with different levels of noise (variable signal-to-noise ratios) and a set of representative noise models and signals.

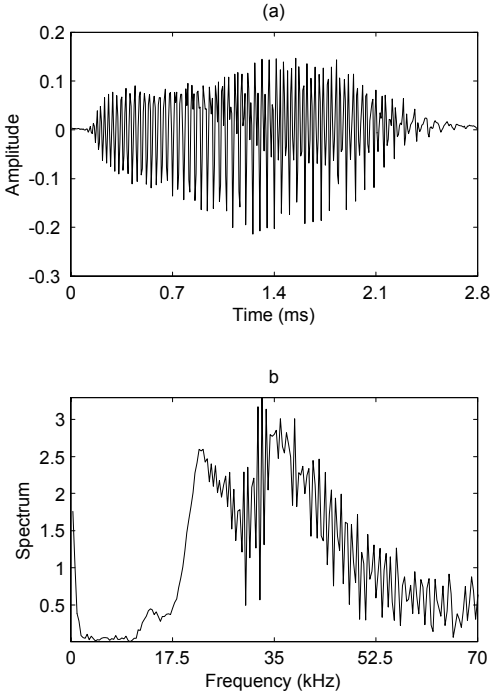

Figure 1: *(a) Time history of bat echolocation signal. (b) Fourier spectrum of bat echolocation signal.*

4. Results and discussion

4.1 Performance evaluation on time-frequency algorithms

In this section we evaluate and compare the qualitative and quantitative performances of different TFDs with an ideal distribution. A TFD maps a one-dimensional signal to a two-dimensional time-frequency image that displays how the frequency content of the signal changes over time. Experimental bat echolocation signals provide an excellent motivation for time-frequency based signal processing. The bats use echolocation signals for navigation and hunting in a dark environment. Bat echolocation signals are high frequency and short duration signals. These signals are made up of chirps having hyperbolic-like instantaneous frequency. For this signal, the frequencies tend to increase with increasing time. The experimental echolocation signal data was taken from [26] and is used for the comparison and evaluation of different TFDs. There are 400 data samples with sampling period of 7 μs. Therefore the data length is 2.8 ms. In this section we evaluate the ability of each TFD to detect the hyperbolic nature of the chirp with minimum artifacts.

Figure 1 shows that neither the time signal nor its Fourier spectrum reveal the true structure of the signal. In contrast, a time-frequency image of the signal clearly exposes its non-stationary character. While each signal has a unique Fourier spectrum, a time-frequency analysis of that signal is not unique. In other words, many different

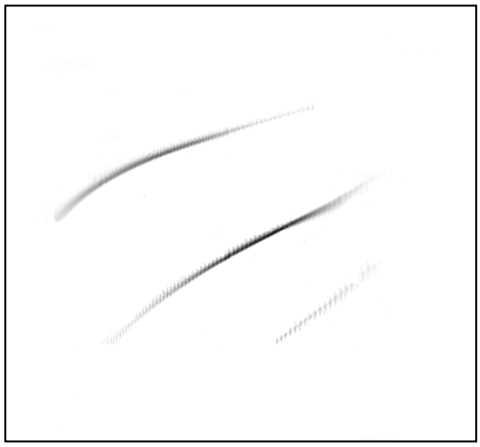

Figure 2: *An ideal time-frequency distribution. The horizontal axis is time and the vertical axis is frequency.*

TFDs can describe the same data. Since for any given signal some TFDs are 'better than others', TFD design has become an important research area.

An ideal distribution or the theoretical instantaneous frequency, i.e., noise-free Wigner-Ville distribution, of a bat echolocation signal is manually plotted in Figure 2 as a reference for comparison. The qualitative performance of different TFDs was examined based on the amount of cross-term artifacts, noise levels and time-frequency resolution (Figures 3-6). The time-frequency resolution of different TFDs was visually compared to the ideal time-frequency distribution. Although we studied and compared all the TFDs described in section 2, we only show certain TFDs in Figures 3-6. However, the quantitative performances of all the TFDs are tabulated in Tables 1-2. The quantitative performance of each TFD was studied using the mean-squared error estimation. The mean-squared error was estimated between TFD produced by each algorithm and an ideal distribution.

Figure 3 shows the adaptive energy distribution and adaptive spectrograms computed by Gabor expansion and Gaussian chirplet decomposition of a bat signal. In this example the time-frequency resolution of the adaptive Gaussian chirplet spectrogram is obviously superior to other two schemes. The adaptive Gaussian chirplet spectrogram not only shows excellent time-frequency resolution, but also does not suffer from cross-term artifacts. Compared with the adaptive energy distribution, the performance of the adaptive Gabor expansion based spectrogram is rather poor. In this case, adaptive Gabor expansion based spectrogram does not offer good time-frequency resolution due to the limitation of the number of degrees of freedom used in the elementary functions. Compared with the adaptive Gabor transform, the adaptive chirplet matches the bat sound much better in terms of fewer terms required. In this case, the adaptive Gabor transform needs 10 times more terms than that needed by its adaptive Gaussian chirplet

Figure 3: *Time-frequency distribution of (a) AED, (b) AGCD and (c) AGE. The horizontal axis is time and the vertical axis is frequency.*

counterpart. This is because the Gaussian chirplet fits the bat sound better than it does the regular Gaussian function. The regular Gaussian function is a special case of the Gaussian chirplet. The adaptive Gaussian chirplet decomposition algorithm is an excellent candidate for signals that are composed of chirps and chirplets, but for signals that have frequency modulation, the adaptive Gaussian chirplet decomposition is not the desired algorithm since it tries to approximate the signal by chirplets (line segments in the TF plane, see Figure 3b).

Figure 4 shows the linear time-frequency transforms with different windows. In this case short-time Fourier transform is used with various window functions. The window functions used in this figure are Gaussian, Hanning and Kaiser. Unlike the adaptive Gaussian chirplet decomposition, these transforms represent all the information contained in the signal. These linear time-frequency transforms often work well, but the performance always depends on the choice of the window used in the representation. In general, the appropriate window depends on the data and can differ for different components in the same signal. Furthermore, selection of the appropriate window requires some knowledge of the signal components of interest. In many applications, such information is not available, and it is desirable to avoid presupposing the form of the data. This is one of the main drawbacks of linear time-frequency transforms.

Figure 5 shows the bilinear TFDs with different kernels. The kernel functions used in this figure are Choi-Williams, tilted Butterworth and tilted Gaussian. These bilinear TFDs generally show better time-frequency resolution than the linear transforms. But these bilinear distributions require longer computational time and have larger amounts of cross-term artifacts. Since real signals have different ambiguity functions, no single kernel can perfectly filter the cross-term artifacts. When a low-pass kernel is employed, there is a trade-off between cross-term suppression and auto-term concentration.

Figure 4: *Linear time-frequency distributions with different windows: (a) Gaussian, (b) Hanning and (c) Kaiser. The horizontal axis is time and the vertical axis is frequency.*

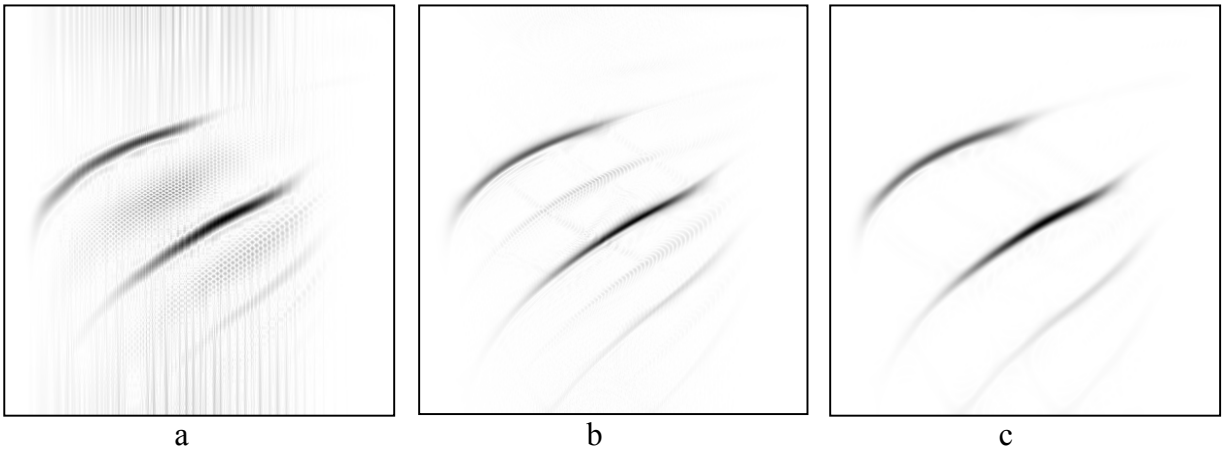

Figure 5: *Bilinear time-frequency distributions with different kernels: (a) Choi-Williams, (b) tilted butterworth and (c) tilted Gaussian. The horizontal axis is time and the vertical axis is frequency.*

Figure 6: *Bilinear time-frequency distributions with adaptive kernels: (a) radially constant, (b) radially Gaussian and (c) radially inverse. The horizontal axis is time and the vertical axis is frequency.*

Generally, as the pass-band region of the kernel reduces, the amount of cross-term artifacts suppression increases, but at the expense of auto-term concentration. Adjustable kernels such as tilted Gaussian and tilted Butterworth can be manually fitted to a signal for better results. However, for some signals, the selection of manual parameters to produce good results is very difficult. Figure 5 shows that the tilted Gaussian kernel function produces the best results in terms of low cross-term artifacts and relatively higher time-frequency resolution than Figures 3-4.

In order to compare the performance of the signal-dependent TFD with the fixed-kernel bilinear TFDs shown in Figure 5, the adaptive optimal kernel TFDs are shown in Figure 6. The kernel functions used in this figure are radially constant, radially Gaussian and radially inverse. Unlike the kernels used in bilinear TFD that emphasize preserving the properties of the Wigner-ville distribution over matching the shape of auto-terms, the signal-dependent kernels aim to optimally pass the auto-terms while suppressing cross-term artifacts. Since a fixed-kernel acts on the ambiguity domain as a filter, it is limited in its ability to perform this function. Figure 6 shows a very good performance for representing a bat sound signal using a signal-dependent kernel. Radially constant (rectangular) and radially inverse kernels have almost as good resolution and as a consequence they produce some ripples or artifacts in the distribution. The radially Gaussian kernel is a good trade-off between the two because it has almost the same resolution and much less artifacts. These results clearly show that the adaptive optimal kernel TFD performs much better than the fixed-kernel methods shown in Figure 5.

The mean-squared error is used as quantitative performance evaluation criterion. Tables 1-2 summarizes the mean-squared errors between the TFDs produced by the algorithms, described in section 2, and an ideal distribution (noise free Wigner-Ville

distribution). As expected, the performance of the adaptive Gaussian chirplet decomposition spectrogram is better than the adaptive Gaussian expansion spectrogram and adaptive energy distribution. Among linear TFDs, most of the window functions such as Hanning, Hamming, Kaiser and Triangular produce similar performance. Generally the bilinear TFDs show better performance than the linear transforms. The tables show that the tilted Gaussian, the Butterworth and the generalized exponential kernel functions produce the good results for bilinear TFDs. Overall, the table clearly shows that the adaptive kernel approach, especially the radially adaptive Gaussian kernel, produces the best results. These results agree with our qualitative assessments (Figures 3-6).

Name of Algorithm	**Additional Parameters**	**MSE**
AED	One iteration	5.4339617e-003
AGCD		2.2599995e-003
AGE		1.2392711e-002
Linear TFDs: (windows length 75)		
Rectangular window		2.8201142e-002
Triangular window		2.3723928e-002
Gaussian window		2.8667000e-002
Inverse window (14)	$p = 0.1$	3.0140008e-002
Inverse window	$p = 0.5$	3.7577926e-002
Hanning window		2.4042926e-002
Hamming window		2.4074127e-002
Kaiser window	$\gamma = \pi$	2.3485069e-002
Kaiser window	$\gamma = 2\pi$	2.4590848e-002
Blackman window		2.6584902e-002
Bilinear TFDs:		
Rectangular (constant) kernel		5.3253611e-003
Born-Jordan kernel		7.6448613e-003
Choi-Williams kernel	$\sigma = 3$	6.1759351e-003
Choi-Williams kernel	$\sigma = 10$	4.4467070e-003
Butterworth kernel	$M = 2, N = 2, \tau_0\theta_0 = 30$	3.4777470e-003
Gaussian kernel	$\sigma = 100$	3.5908155e-003
Gaussian kernel	$\sigma = 200$	6.2000926e-003
Generalized exponential distribution	$M = 10, N = 1, \tau_0\theta_0 = 30$	2.1118777e-003
Generalized exponential distribution	$M = 5, N = 2, \tau_0\theta_0 = 50$	1.6623236e-003
Cone-shaped kernel	$\alpha = 0.001$	6.8324434e-003
Cone-shaped kernel	$\alpha = 0.0001$	6.7897483e-003
Tilted Gaussian distribution	$\tau_0 = 0.1, \theta_0 = 0.2, r = 0.5$	1.9228440e-003
Tilted Gaussian distribution	$\tau_0 = 0.2, \theta_0 = 0.1, r = 0.5$	8.1887901e-003
Tilted Butterworth distribution	$\tau_0 = 0.05, \theta_0 = 0.1, r = 0.5$	1.1315364e-003
Tilted Butterworth distribution	$\tau_0 = 0.1, \theta_0 = 0.2, r = 0.5$	8.8955521e-004

Table 1: *Quantitative performance evaluation of TFDs*

Name of Algorithm	**Additional Parameters**	**MSE**
Adaptive kernel: radially constant	$\sigma(\psi) = 100$	1.0445602e-003
Adaptive kernel: radially constant	$\sigma(\psi) = 200$	6.9237386e-004
Adaptive kernel: radially Gaussian	$\sigma(\psi) = 100$	8.8654181e-004
Adaptive kernel: radially Gaussian	$\sigma(\psi) = 200$	6.2966003e-004
Adaptive kernel: radially inverse	$\sigma(\psi) = 100$	1.9123454e-003
Adaptive kernel: radially inverse	$\sigma(\psi) = 200$	1.0593200e-003

Table 2: *Quantitative performance evaluation of TFDs*

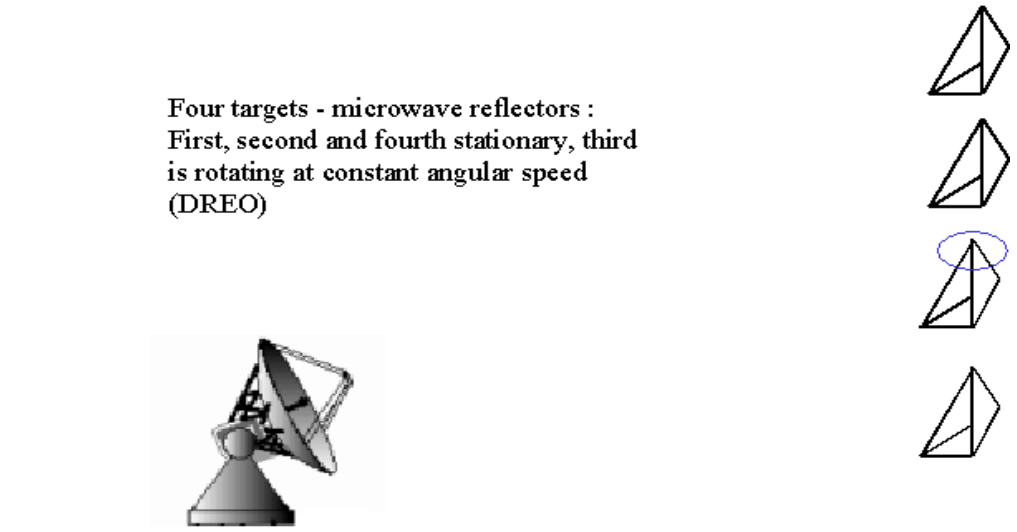

Figure 7: *A schematic of the experiment set-up for studying an oscillating scatterer. The third scatterer from the top is attached to a mechanical sine-drive. The other three scatterers are stationary to provide reference in the HRR profiles.*

4.2 Fusion approach

We demonstrate the performance of our new algorithm using the experimental high range resolution radar data. An experiment was set up to compare the new TFD approach with other available TFDs. High range resolution profiles were collected using a stepped frequency wave-form (SFWF) radar mode at X-band between 8.9 to 9.3 GHz., i.e., a synthetic bandwidth of 400 MHz; the frequency step size was 1 MHz. The experimental set up is shown schematically in Figure 7, which shows the three stationary corner reflectors and an oscillating corner reflector. The test target was made up of four corner reflectors, three of which are stationary to provide a geometric reference and a contrast to the distorting shape of the oscillating reflector in the HRR profiles.

Figure 8 shows the standard HRR image of the complex target. The HRR profile of an oscillating scatterer is clearly apparent in the figure. When the oscillating scatterer is stationary, a sharp peak is observed in the HRR profile as expected. This is shown as the top profile in Figure 8. However, when the scatterer is in motion, the spread in the spectrum tells us very little about the scatterer's bahaviour, as shown as the bottom profile in Figure 8.

TFDs immediately provide more information. Figure 9 shows the time-frequency signature of the radar signal returned from the four scatterers, where the oscillating curve can be observed very well. Figure 9 shows the results of nine TFDs. TFDs used in this figure are Wigner-Ville distribution, Born-Jordan distribution, Choi-Williams

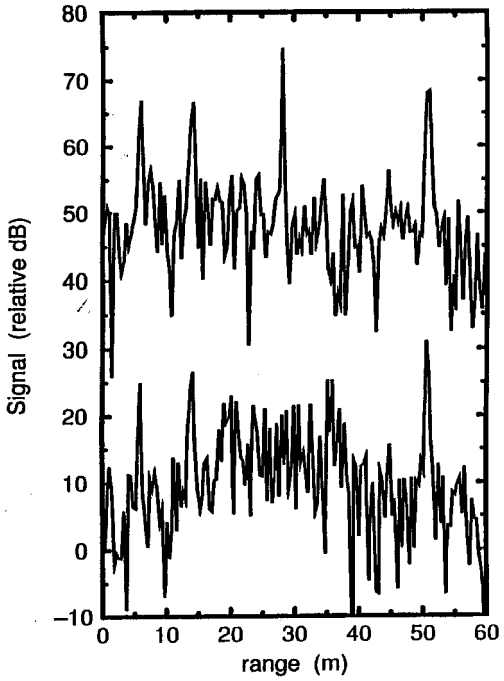

Figure 8: *HRR profiles of four-scatterer target. Top profile: all four scatterers stationary; bottom profile: three stationary scatterers and one oscillating scatterer.*

distribution, bilinear TFD with Butterworth kernel, bilinear TFD with 2-dimensional Gaussian kernel, generalized exponential distribution, cone-shaped distribution, tilted Gaussian distribution and tilted Butterworth distribution. These nine TFDs are used for the algorithmic fusion method described in Section 4. Figure 10 shows the resulting TFD obtained by using the algorithmic fusion method. An ideal distribution, i.e., noise-free Wigner-Ville distribution, is manually plotted in Figure 11 as a reference for comparison. As expected, Figure 10 shows considerable improvement over other TFDs presented in Figure 9. We can see that Figure 10 achieves the same sharpness as the reference image. These results demonstrate that the new algorithmic fusion method performed well in achieving improved resolution, highly concentrated and readable representation, without the auto-term distortion and cross-term artifacts that are apparent in all the representations of Figure 9.

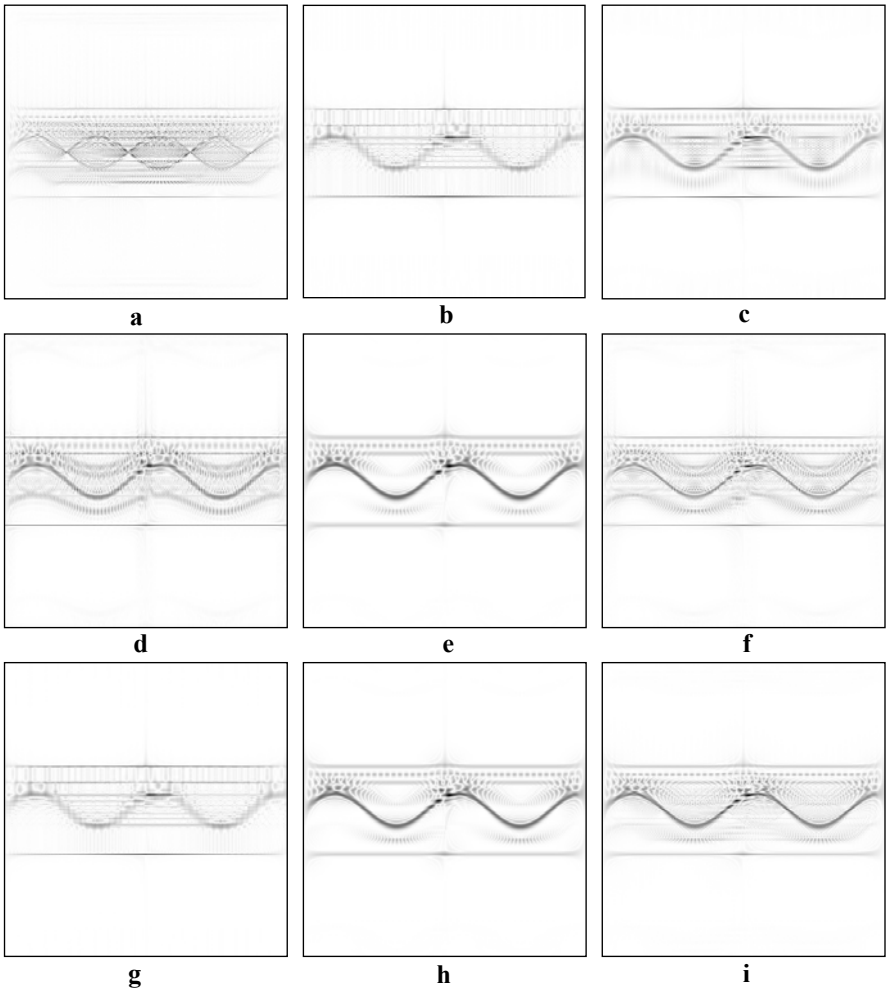

Figure 9: *Results of nine TFDs: (a) Wigner-Ville distribution, (b) Born-Jordan distribution, (c) Choi-Williams distribution, (d) bilinear TFD with Butterworth kernel, (e) bilinear TFD with 2-dimensional Gaussian kernel, (f) generalized exponential distribution, (g) cone-shaped distribution, tilted Gaussian distribution and (h) tilted Butterworth distribution. The horizontal axis is time and the vertical axis is frequency.*

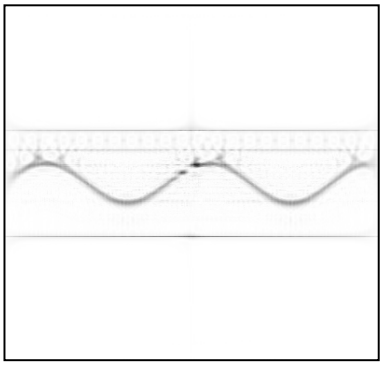

Figure 10: *TFD obtained from the algorithmic fusion method. The horizontal axis is time and the vertical axis is frequency.*

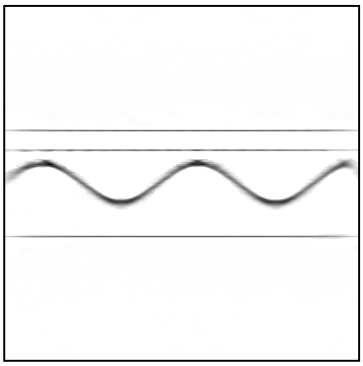

Figure 11: *An ideal time-frequency distribution. The horizontal axis is time and the vertical axis is frequency.*

5. Conclusion

This report evaluates and compares the qualitative and quantitative performances of different time-frequency distributions (TFDs) developed for the past ten years and proposes a new approach in time-frequency analysis applied to synthetic aperture radar imaging and target feature analysis.

Among linear TFDs, most of the window functions such as Hanning, Hamming, Kaiser and Triangular produce similar performance. Generally the bilinear TFDs show better performance than the linear transforms. The tilted Gaussian, the Butterworth and the generalized exponential kernel functions produce good results for bilinear TFDs. The performance of the adaptive Gaussian chirplet decomposition spectrogram is better than the adaptive Gaussian expansion spectrogram and adaptive energy distribution. Overall, the study clearly shows that the adaptive kernel approach, especially the radially adaptive Gaussian kernel, produces the best results from all tested methods when the mean-squared error is used as the performance evaluation criterion. These results agree with our qualitative assessments. A short review of different time-frequency approaches is also provided.

A new TFD algorithmic fusion method is presented and evaluated on the experimental high range resolution radar data and simulated data. It is shown that the TFD algorithmic fusion method provides an effective method of achieving improved resolution, highly concentrated and readable representation without the auto-term distortion and cross-term artifacts. This method is suitable for HRR and ISAR data where multiple scatterers are present, and noise along with artifact reduction are essential for target identification applications. Analysis of the time-varying Doppler signature in the joint time-frequency domain can provide useful information for target detection, classification and recognition. We anticipate that this new approach will find a wide range of uses and will emerge as a powerful tool for time-varying spectral analysis.

Our study shows how the TFD algorithmic fusion method provides useful data visualization of non-stationary signals in the time-frequency plane. For useful application of this method, however, the derivation of measures, statistics, or parameters from the time-frequency plane, are required for further analysis and processing; for example, automated target detection and classification. This is the essential step to enable TFD algorithmic fusion method to be employed for processing tasks other than data display. One of the advantages of the TFD algorithmic fusion approach is that the noise tends to spread out its energy over the entire time-frequency domain, while target signals often concentrate their energy on regions with limited time intervals and frequency bands. Thus, signals embedded in noise are much easier to recognize in the joint time-frequency domain. Hence, with constant false-alarm rate (CFAR) detection, signals can be detected and reconstructed by using only the detected time-frequency coefficients. Therefore, the target signal buried in noise can be detected and its parameters can be measured. By applying time-varying frequency filtering, the

signal-to-noise ratio (SNR) can also be enhanced and the resulting statistics would outperform the conventional measure. We intend to investigate these scenarios in the future study.

Another significant advantage of the TFD algorithmic fusion method, as we have already seen, is that it allows us to determine whether, or not, a signal is multicomponent or not and its ability to decompose the signal in the time-frequency plane. That is, the time-frequency analysis enables us to classify signals with a considerably greater reflection of the physical situation than can be achieved by the Fourier spectrum alone. Based on this time-frequency localization, one may wish to select "desired" signal components and remove unwanted contributions, by applying an appropriate mask function. Time-varying filtering and signal synthesis have been applied to many signal processing areas and we intend to investigate these approaches in our future study.

This work is especially relevant to the HRR/ISAR imaging capability of the surveillance radar systems on-board of the CF C-140 Aurora patrol aircraft and the US Navy's P3 Orion surveillance aircraft. Moreover, target recognition based on radar imagery will play an active role in future CF initiatives on ISR (Intelligence, Surveillance and Reconnaissance) for land, air and maritime applications.

References

1. Wong, S. K., Duff, G., and Riseborough, E. (2001). Analysis of distortion in the high range resolution profile from a perturbed target, *IEE Proc.-Radar, Sonar Navig.*, vol 148, pp. 353-362

2. Yasotharan, T. and Thayaparan, T. (2002). Strengths and Limitation of the Fourier method for detecting accelerating targets by pulse Doppler radar, *IEE Proceedings - Radar Sonar Navig.*, vol. 149, pp. 83-88.

3. Thayaparan, T. (2000). Limitation and Strengths of the Fourier transform method to detect accelerating targets, *Defence Research Establishment Ottawa*, DREO TM 2000-078.

4. Qian, S. (2002). Time-frequency and wavelet transforms, *Prentice-Hall Inc.,* New York, USA.

5. Cohen, L. (1989). Time-Frequency Distributions - A Review, *Proc. IEEE,* vol. 77, pp. 941-981 1989.

6. Cohen, L. (1995). Time-frequency analysis, *Prentice-Hall Inc.,* New York, USA.

7. Hlawatsch, F. and Boudreaux-Bartels, G.F., Linear and Quadratic Time- Frequency Signal Representations, *IEEE Signal Processing Magazine*, April, 1992.

8. Chen, V. C. and Ling, H. (2002). Time-Frequency Transforms for Radar Imagine and Signal Analysis, *Artech House*, Boston, MA, USA.

9. Qian, S. and Chen, D. (1996). Joint time-frequency analysis: methods and applications, *Prentice-Hall Inc.,* New York, USA.

10. Thayaparan, T. (2000). Linear and quadratic time-frequency representations, *Defence Research Establishment Ottawa*, DREO TM 2000-080.

11. Cohen, L. (1966). Generalized phase-space distribution functions, *J. Math. Phys.*, vol. 7. pp. 781-786.

12. Claasen, T. A. C. M. and Mecklenbräuker, W. F. G. (1980). The Wigner distribution - a tool for time-frequency signal analysis - part III: Relations with other time-frequency signal transformation, *Philips Jour. Research.*, vol. 35, pp. 372-389.

13. Choi, H. and Williams, W. (1989). Improved time-frequency representation of multicomponent signals using exponential kernels, *IEEE Trans. on Acoustics, Speech and Signal Processing*, vol. 37, pp. 862-871.

14. Mann, S. and Haykin, S. (1991). The Chirplet Transform: a Generalization of Gabor's Logon Transform, Vision Interface 1991, *Canadian Image Processing and Pattern Recognition Society*, June 3-7, pp. 205-212.

15. Yin, Q., Qian, S. and Feng, A. (2002). A fast refinement for adaptive Gaussian chirplet decomposition, *IEEE Transactions on signal processing*, vol. 50, pp. 1298-1306.

16. Stockwell, R. G., Lowe, R. and Mansinha, L. (1996). Localization of complex spectrum: the s-transform, *IEEE Transactions on signal processing*, vol. 44, pp. 998-1001.

17. Mansinha, L. Stockwell, R. G., Lowe, R. P., Eramian M. and Shincariol, R. A. (1997). Local S-spectrum analysis of 1-D and 2-D data, Elsevier Science, *Physics of the Earth and Planetary Interiors 103*, pp. 329-336.

18. Chen, V. C. and Ling, H. (1999). Radar Signal and Image Processing: Applying JTF analysis to radar backscattering, feature extraction, and imaging of moving targets, *IEEE Signal Processing Magazine*, pp. 81-93.

19. Chen, V. C. and Qian, S. (1998). Joint Time-Frequency Transform for Radar Range-Doppler Imaging, *IEEE Transactions on Aerospace and Electronic Systems*, Vol. 34, pp. 486-499.

20. Auger, F. and Flandrin, P. (1995). Improving the readability of time-frequency and time-scale representations by the reassignment method, *IEEE Transactions on Signal Processing*, vol. 43, pp. 1068-1089.

21. Auger, F., Flandrin, P., Gonçalvès, P. and Lemoine, O. (1995). Time-frequency toolbox tutorial, *Rice University*, USA.

22. Jones, G. and Boashash, B. (1997). Generalized instantaneous parameters and window matching in the time-frequency plane, *IEEE Transactions on Signal Processing*, vol. 45, pp. 1264-1275.

23. Thayaparan, T. and Yasotharan, A. (2002). Application of Wigner distribution for the detection of accelerating low-altitude aircraft using HF surface-wave radar, *Defence Research Establishment Ottawa*, DREO TR 2002-033.

24. Thayaparan, T. and Yasotharan, A. (2002). A noval approach for the wigner distribution formulation of the optimum detection problem for a discrete-time chirp signal, *Defence Research Establishment Ottawa*, DREO TR 2001-141.

25. Jones, D. L. and Baraniuk, R. G. (1995). An adaptive optimal-kernel time-frequency representation, *IEEE Transactions on Signal Processing*, vol. 43, pp. 2361-2371.

26. http://www.dsp.rise.edu/software/bat.html

DOCUMENT CONTROL DATA

(Security classification of title, body of abstract and indexing annotation must be entered when the overall document is classified)

1. ORIGINATOR (the name and address of the organization preparing the document. Organizations for whom the document was prepared, e.g. Establishment sponsoring a contractor's report, or tasking agency, are entered in section 8.)

Defence R&D Canada - Ottawa
Ottawa, Ontario, Canada K1A 0Z4

2. SECURITY CLASSIFICATION (overall security classification of the document, including special warning terms if applicable)

UNCLASSIFIED

3. TITLE (the complete document title as indicated on the title page. Its classification should be indicated by the appropriate abbreviation (S,C or U) in parentheses after the title.)

A New Approach in Time-Frequency Analysis with Applications to Experimental High Range Resolution Radar Data (U)

4. AUTHORS (Last name, first name, middle initial)

Thayaparan, Thayananthan; Lampropoulos, George

5. DATE OF PUBLICATION (month and year of publication of document)	6a. NO. OF PAGES (total containing information. Include Annexes, Appendices, etc.)	6b. NO. OF REFS (total cited in document)
November 2003	39	26

7. DESCRIPTIVE NOTES (the category of the document, e.g. technical report, technical note or memorandum. If appropriate, enter the type of report, e.g. interim, progress, summary, annual or final. Give the inclusive dates when a specific reporting period is covered.)

DRDC Ottawa Technical Report

8. SPONSORING ACTIVITY (the name of the department project office or laboratory sponsoring the research and development. Include the address.)

Defence R&D Canada - Ottawa
Ottawa, Ontario, Canada K1A 0Z4

9a. PROJECT OR GRANT NO. (if appropriate, the applicable research and development project or grant number under which the document was written. Please specify whether project or grant)	9b. CONTRACT NO. (if appropriate, the applicable number under which the document was written)
11ar16	

10a. ORIGINATOR'S DOCUMENT NUMBER (the official document number by which the document is identified by the originating activity. This number must be unique to this document.)	10b. OTHER DOCUMENT NOS. (Any other numbers which may be assigned this document either by the originator or by the sponsor)
DRDC Ottawa TR 2003-187	

11. DOCUMENT AVAILABILITY (any limitations on further dissemination of the document, other than those imposed by security classification)

(X) Unlimited distribution
( ) Distribution limited to defence departments and defence contractors; further distribution only as approved
( ) Distribution limited to defence departments and Canadian defence contractors; further distribution only as approved
( ) Distribution limited to government departments and agencies; further distribution only as approved
( ) Distribution limited to defence departments; further distribution only as approved
( ) Other (please specify):

12. DOCUMENT ANNOUNCEMENT (any limitation to the bibliographic announcement of this document. This will normally correspond to the Document Availability (11). However, where further distribution (beyond the audience specified in 11) is possible, a wider announcement audience may be selected.)

13. ABSTRACT (a brief and factual summary of the document. It may also appear elsewhere in the body of the document itself. It is highly desirable that the abstract of classified documents be unclassified. Each paragraph of the abstract shall begin with an indication of the security classification of the information in the paragraph (unless the document itself is unclassified) represented as (S), (C), or (U). It is not necessary to include here abstracts in both official languages unless the text is bilingual).

(U) This report presents trade-off studies on Time-Frequency Distribution (TFD) algorithms and a methodology for fusing them to achieve better target characterization. It is shown that TFD algorithmic fusion considerably increases the detectability of signals while suppressing artifacts and noise. The report reviews a sample of representative TFD algorithms. Their performance is studied from a qualitative and quantitative point of view. For simplicity, we considered the mean-squared error as a measure of performance in the quantitative trade-off studies. The TFD algorithmic fusion is performed using a self-adaptive signal. It may be adjusted to work for a wide range of signal-to noise ratios. The algorithm uses the first two terms of the Volterra series expansion and we treat the outputs of the time-frequency algorithms as the variables of a Volterra series and the coefficients of the series are estimated through training sets with a least-squares algorithm. Simplistic TFD algorithmic fusion methods (e.g., weighted averaging or weighted multiplication) are special cases of the proposed fusion technique. We demonstrate the effectiveness of TFD algorithmic fusion method using experimental High Range Resolution (HRR) radar data.

14. KEYWORDS, DESCRIPTORS or IDENTIFIERS (technically meaningful terms or short phrases that characterize a document and could be helpful in cataloguing the document. They should be selected so that no security classification is required. Identifiers such as equipment model designation, trade name, military project code name, geographic location may also be included. If possible keywords should be selected from a published thesaurus. e.g. Thesaurus of Engineering and Scientific Terms (TEST) and that thesaurus-identified. If it is not possible to select indexing terms which are Unclassified, the classification of each should be indicated as with the title.)

Time-Frequency Distribution
High Range Resolution
Inverse Synthetic Aperture Radar
Algorithmic Fusion
Non-Cooperative Target Recognition
Fourier Transform
Doppler Smearing
ISAR image
Adaptive Energy Distribution
Adaptive Gaussian Chirplet Decomposition
Adaptive Gabor Expansion
Linear Time-frequency Transforms
Bilinear Time-Frequency Distributions
Adaptive Optimal Kernel
Volterra Series

Defence R&D Canada

Canada's leader in defence
and national security R&D

R & D pour la défense Canada

Chef de file au Canada en R & D
pour la défense et la sécurité nationale

www.drdc-rddc.gc.ca